Wireless Pers Commun (2011) 58:695–711
DOI 10.1007/s11277-009-9902-1

A N-Radon Based OFDM Trasceivers Design and Performance Simulation Over Different Channel Models

Abbas Hasan Kattoush · Waleed Ameen Mahmoud Al-Jawher · Sulaiman M. Abbas · Ali Tweij Shaheen

Published online: 25 December 2009

Abstract In this paper a new method is proposed to perform the N-Radon orthogonal frequency division multiplexing (OFDM), which are equivalent to 4-quadrature amplitude modulation (QAM), 16-QAM, 64-QAM, 256-QAM, … etc. in spectral efficiency. This non conventional method is proposed in order to reduce the constellation energy and increase spectral efficiency. The proposed method gives a significant improvement in Bit Error Rate performance, and keeps bandwidth efficiency and spectrum shape as good as conventional Fast Fourier Transform based OFDM. The new structure was tested and compared with conventional OFDM for Additive White Gaussian Noise, flat, and multi-path selective fading channels. Simulation tests were generated for different channels parameters values including multi-path gains vector, multi-path delay time vector, and maximum Doppler shift.

Keywords Finite Radon transform · Data mapping · OFDM · N-Radon-based OFDM transceiver

1 Introduction

Orthogonal frequency division multiplexing (OFDM) system is one of the most promising technologies for current and future wireless communications [1]. It is a form of multi-carrier modulation technologies [2,3] where data bits are encoded to multiple sub-carriers, while being sent simultaneously. Each sub-carrier in an OFDM system is modulated in amplitude and phase by the data bits. Modulation techniques typically used are binary phase shift keying,

A. H. Kattoush (✉)
EE Department, Tafila Technical University, Tafila, Jordan
e-mail: akattoush@yahoo.ca

W. A. M. Al-Jawher
Al-Isra University, Amman, Jordan

S. M. Abbas · A. T. Shaheen
EE Department, Baghdad University-IRAQ, Baghdad, Iraq

quadrature phase shift keying (QPSK), 16-QAM, 64-QAM etc. The process of combining different sub-carriers to form a composite time-domain signal is achieved using Fast Fourier Transform (FFT) and inverse FFT (IFFT) operations [4].

The main problem in the design of a communications system over a wireless link is to deal with multi-path fading, which causes a significant degradation in terms of both the reliability of the link and the data rate [5]. Multi-path fading channels have a severe effect on the performance of wireless communication systems even those systems that exhibits efficient bandwidth, like OFDM [6]. There is always a need for developments in the realization of these systems as well as efficient channel estimation and equalization methods to enable these systems to reach their maximum performance [7]. The OFDM receiver structure allows relatively straightforward signal processing to combat channel delay spreads, which was a prime motivation to use OFDM modulation methods in several standards [8–12].

In transmissions over a radio channel, the orthogonality of the signals is maintained only if the channel is flat and time-invariant, channels with a Doppler spread and the corresponding time variations corrupt the orthogonality of the OFDM sub-carrier waveforms [13]. In a dispersive channel, self-interference occurs among successive symbols at the same sub-carrier casing inter symbol interference (ISI), as well as among signals at different sub-carriers casing inter carrier interference (ICI). For a time-invariant but frequency-selective channel, ICI, as well as ISI, can effectively be avoided by inserting a cyclic prefix before each block of parallel data symbols at the cost of power loss and bandwidth expansion [4]. Some solutions for ICI mitigation, such as pre-coding for self-cancellation [14], require a modification of the transmit format so that these are not suitable for existing standards [15]. Other techniques are compatible with existing transmit schemes, but may not be suitable for high vehicle speeds or become too complex for consumer products.

The Radon transform (RT) was first introduced by Johann Radon (1917) and the theory, basic aspects, and applications of this transform are studied in [16,17] while the finite Radon transform (FRAT) was first studied by [18]. RT is the underlying fundamental concept used for computerized tomography scanning, as well for a wide range of other disciplines, including radar imaging, geophysical imaging, nondestructive testing and medical imaging [16]. The enormous growth in the application areas of the Radon Transform and the fact that digital computations are often required, has led to the development of the Discrete Radon Transform (DRT). The Radon transform is a widely studied algorithm used to perform image pattern extraction in fields such as computer graphics and several others digital signal and image processing applications [19–23].

In this paper a new application for Finite Radon Transform (FRAT) is proposed. The idea of one dimensional serial Radon based OFDM proposed in [24] is develop farther to words increasing spectral efficiency and reducing the constellation energy.

2 Radon Transform, Inverse Radon Transform, and Finite Radon Transform

Let (x, y) designate coordinates of points in the Cartesian plane, and consider some arbitrary function f defined on some domain D on R^2. If L is any line in the plane, then the mapping defined by the projection or line integral of f along all the possible lines L is the (two-dimensional) Radon transform of f provided that the integral exists. Explicitly,

$$\breve{f} = \mathcal{R}f = \int_L f(x, y)ds \tag{1}$$

Where, ds is an increment of length along L. The domain D may include the entire plane or some region of the plane as shown in Fig. 1.

The mapping defined by Eq. (1) along with its inverse and certain generalizations, was studied first by Johann Radon (1917) [25]. Radon showed that if f is continuous, then $\Re f is$ uniquely determined by integrating along all the lines L.

There are many approaches to recover function f from its RT version $\breve{f}$ [16,26], Fourier Transform (FT) method of Inverse Radon Transform (IRT) will be used through out this paper. The fundamental connection between FT and RT is established through the following equation [16]:

$$\tilde{f} = \mathcal{F}_1 \breve{f} = F_1 \mathcal{R} f \tag{2}$$

where: F_1- one-dimensional FT, $\tilde{f}$- FT of f function.

Figure 2 clarifies this connection diagrammatically. In effect $\breve{f}$ maybe obtained by applying the inverse FT in the radial direction once $\tilde{f}$ is known. Symbolically,

$$\mathcal{R} f = \mathcal{F}^{-1} \mathcal{F}_n f \tag{3}$$

The diagrammatic interpretation of Eq. (3) is shown in Fig. 3. Thus, given $\breve{f}$ it is possible to recover f by a radial FT followed by n-dimensional inverse FT. Symbolically,

$$f = \mathcal{F}_n^{-1} \mathcal{F}_1 \breve{f} \tag{4}$$

Fig. 1 *Line* L through domain D

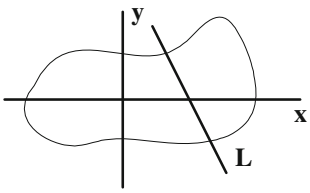

Fig. 2 Relation between RT and FT

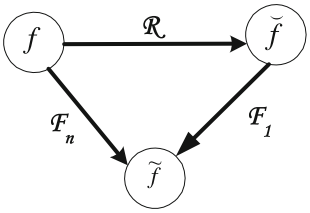

Fig. 3 Diagrammatic interpretation of Eq. (3)

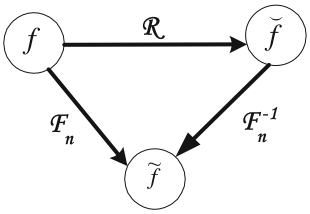

FRAT was defined for two dimensional (2D) images in [17,18]. In this paper, the FT approach will be used due to its suitability for our purposes. The FRAT of a two dimensional matrix A can be obtained first by taking the 2D-FFT of A [17,26]:

$$F(r,s) = \sum_{m=0}^{p-1} \sum_{n=0}^{p-1} A(m,n)\, e^{-j(2\pi/p)rm}\, e^{-j(2\pi/p)ns} \tag{5}$$

Then the order of coefficients in the corresponding Fourier slices are controlled by the direction of a set of normal vectors, namely (a_k, b_k), where $k = 0, 1, 2, \ldots, p$. These normal vectors refer to the row and column indices in the Fourier domain. The optimal ordering of Radon coefficients was suggested first in [25]. It was shown that the optimum number of FRAT projections is $p + 1$, one projection for each column, and the best ordering of the 2D-FFT coefficients in these projections which is controlled by the normal vectors can be achieved if the normal vectors determined as [16]:

$$\begin{aligned} &(a_k, b_k) = \arg\min \left| \left(\mathrm{C_p}(a_k), \mathrm{C_p}(b_k)\right) \right| \\ &(a_k, b_k) \in \{nu_k : 1 \le n \le p-1\} \\ &st.C_p(b_k) \ge 0 \end{aligned} \tag{6}$$

Here $C_p(x)$ denotes the centralized function of period p; $C_p(x) = x - p.round(x/p)$. Hence, $\left\| (C_p(a_k), C_p(b_k)) \right\|$ represents the distance from the origin to the point (a_k, b_k) on the Fourier plane. The constraint $C_p(b_k) \ge 0$ is imposed in order to remove the ambiguity in deciding between (a, b) and $(-a, -b)$ as the normal vector for the projection. As a result the optimal normal vectors are restricted to have angles in $[0, \pi)$ and reordered matrix F is assigned symbol $\mathcal{F}_{opt}$. Matrixes $\mathcal{F}$ and $\mathcal{F}_{opt}$ for $p = 7$ are given by Eqs. (7) and (8) respectively:

$$\mathcal{F} = \begin{bmatrix} f_1 & f_8 & f_{15} & f_{22} & f_{29} & f_{36} & f_{43} \\ f_2 & f_9 & f_{16} & f_{23} & f_{30} & f_{37} & f_{44} \\ f_3 & f_{10} & f_{17} & f_{24} & f_{31} & f_{38} & f_{45} \\ f_4 & f_{11} & f_{18} & f_{25} & f_{32} & f_{39} & f_{46} \\ f_5 & f_{12} & f_{19} & f_{26} & f_{33} & f_{40} & f_{47} \\ f_6 & f_{13} & f_{20} & f_{27} & f_{34} & f_{41} & f_{48} \\ f_7 & f_{14} & f_{21} & f_{28} & f_{35} & f_{42} & f_{49} \end{bmatrix} \tag{7}$$

$$\mathcal{F}_{opt} = \begin{bmatrix} f_1 & f_1 & f_1 & f_1 & f_1 & f_1 & f_1 & f_1 \\ f_2 & f_{10} & f_9 & f_{16} & f_8 & f_{21} & f_{14} & f_{13} \\ f_3 & f_{19} & f_{17} & f_{31} & f_{15} & f_{34} & f_{20} & f_{18} \\ f_4 & f_{28} & f_{25} & f_{46} & f_{22} & f_{47} & f_{26} & f_{23} \\ f_5 & f_{30} & f_{33} & f_{12} & f_{29} & f_{11} & f_{32} & f_{35} \\ f_6 & f_{39} & f_{41} & f_{27} & f_{36} & f_{24} & f_{38} & f_{40} \\ f_7 & f_{48} & f_{49} & f_{42} & f_{43} & f_{37} & f_{44} & f_{45} \end{bmatrix} \tag{8}$$

Finally, FRAT can be obtained by taking the one dimensional (1D) IFFT for each column of the matrix $\mathcal{F}_{opt}$. So, if the columns of the matrix $\mathcal{F}_{opt}$ are assigned the symbol f_i, where i takes the values of 0, 1, 2, 3, ..., p, [25] then:

$$r_i(k) = Re\left\{ \frac{1}{p} \sum_{m=0}^{p-1} f(i) e^{j(2\pi/p)km} \right\} \tag{9}$$

Now, the matrix with the $r(i)$ columns represents the FRAT of A:

$$\Re = [r(1)r(2)r(3)\cdots r(p)] \tag{10}$$

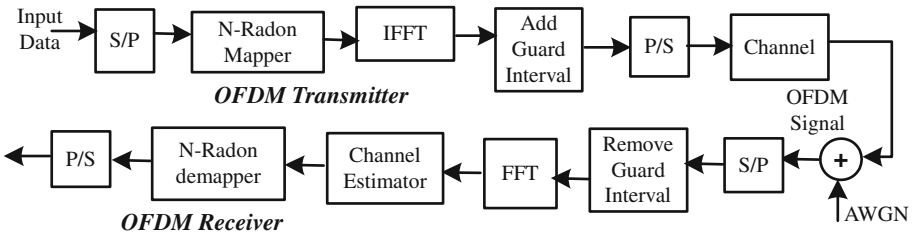

Fig. 4 Proposed N-Radon based OFDM transceiver

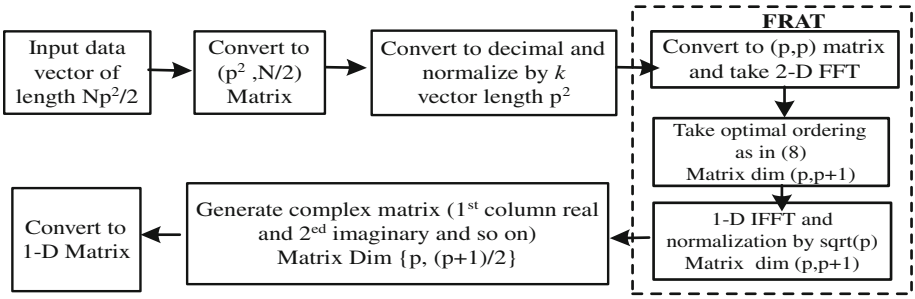

Fig. 5 Proposed N-Radon mapper

Also [25] showed that normalization by the square root of the matrix size, p leads to better performance. Matrix A can be recovered by reversing the above procedure (taking 1D FFT, retrieving original Fourier coefficients ordering, and then taking 2D-IFFT).

3 Proposed N-Radon Based OFDM Transceiver

In this section we propose and describe a general technique for N-Radon-based OFDM where $N = 2, 4, 6, 8, 10\ldots$ etc. which is equivalent to 4-QAM, 16-QAM, 64-QAM, 256-QAM, 1024-QAM etc. The block diagram of proposed N-Radon based OFDM transceiver is similar to that of conventional OFDM transceiver as shown in Fig. 4. Instead of QAM mapper used in conventional OFDM, a new Radon transform mapper is implemented in this design. It works as a good interleaver and provides a high immunity against ICI due to implementation of IFFT twice: in the mapper and in the sub-carrier modulation. As a result, proposed system gives a significant reduction in Bit Error Rate (BER) as compared with conventional 16-QAM and 64-QAM based OFDM systems. Another important result obtained here is that, proposed N-Radon mapper has constellation of very small energy as compared with that of QAM mapper.

The N-Radon mapping procedure block diagram is shown in Fig. 5. In this procedure p is a prime number and N is an even number. The procedure follows the following steps:

Step 1. Take column vector of length $(N/2)\ p^2$ of input binary data. If $p = 3$, then for 2-Radon case the vector length is 9 bits, 4-Radon case 18 bits, 6-Radon case 27 bits, … etc.

Step 2. Convert the column vector of step1 to 2D matrix of dimension $\left(p^2, N/2\right)$. In the case of 2-Radon the vector is not changed since the matrix dimension (9, 1) is a column vector. For the 4-Radon case the matrix dimension is (9, 2) and so on.

Step 3. Convert the matrix data in Step 2 from binary to decimal to obtain a column vector of decimal data with length (p^2), all elements in this vector are between (0 and $2^{N/2}-1$). Then normalize this data vector by dividing it by $k=\sqrt{2^{N/2}-1}$. The new vector elements will be between (0 and $\sqrt{2^{N/2}-1}$).

Step 4. Convert the vector in Step3 to 2D matrix $D(k)$of dimension (p, p). Suppose that data bits at the input of 4-Radon are (1001101100101011 00), then for 4-Radon mapping the matrixes after Step 2, Step 3, and Step 4 are:

$$(1001101100101011 00) \Rightarrow \begin{bmatrix} 1 & 0 \\ 0 & 1 \\ 0 & 0 \\ 1 & 1 \\ 1 & 0 \\ 0 & 1 \\ 1 & 1 \\ 1 & 0 \\ 0 & 0 \end{bmatrix} \Rightarrow \begin{bmatrix} 2 \\ 1 \\ 0 \\ 3 \\ 2 \\ 1 \\ 3 \\ 2 \\ 0 \end{bmatrix} \Rightarrow \begin{bmatrix} 2/\sqrt{3} \\ 1/\sqrt{3} \\ 0 \\ \sqrt{3} \\ 2/\sqrt{3} \\ 1/\sqrt{3} \\ \sqrt{3} \\ 2/\sqrt{3} \\ 0 \end{bmatrix} \Rightarrow D(k)$$

$$= \begin{bmatrix} 2/\sqrt{3} & \sqrt{3} & \sqrt{3} \\ 1/\sqrt{3} & 2/\sqrt{3} & 2/\sqrt{3} \\ 0 & 1/\sqrt{3} & 0 \end{bmatrix}$$

Then take Radon transform (Step 5, Step 6, and Step 7) as shown in Fig. 5 to obtain a new matrix of dimension $(p, p+1)$.

Step 5. Take the 2-D FFT of the matrix $D(k)$ to obtain the matrix, $F(r, s)$ given by Eq. (5). For simplicity it will be labeled by$F$.

Step 6. Redistribute the elements of the matrix F according to the optimum ordering algorithm given in [25]. So, the dimensions of the resultant matrix will be $p \times (p+1)$ and will be denoted by symbol $\mathcal{F}_{opt}$. The two matrixes for FRAT window= 7 are given by Eqs. (7) and (8).

Step 7. Take 1D-IFFT for each column of the matrix $\mathcal{F}_{opt}$ to obtain the matrix of Radon coefficients, R:

$$R = \frac{1}{p} \sum_{k=0}^{N-1} F_{opt} e^{(j2\pi kn/p)} \tag{11}$$

Step 8. Construct the complex matrix $\overline{R}$ from the real matrix R such that its dimensions will be $p \times (p+1)/2$ according to:

$$\overline{r_{l,m}} = r_{i,j} + j r_{i,j+1}, \quad 0 \le i \le p, 0 \le j \le p, \tag{12}$$

Where, $\overline{r_{l,m}}$ refers to the elements of the matrix$\overline{R}$, while $r_{i,j}$ refers to the elements of the matrix R. Matrixes R and $\overline{R}$ are given by:

$$\mathcal{R} = \begin{bmatrix} r_{1,1} & r_{1,2} & r_{1,3} & \cdots\cdots & r_{1,p+1} \\ r_{2,1} & r_{2,2} & r_{2,3} & \cdots\cdots & r_{2,p+1} \\ \vdots & \vdots & \vdots & \cdots\cdots & \vdots \\ \vdots & \vdots & \vdots & \cdots\cdots & \vdots \\ r_{p-1,1} & r_{p-1,2} & \cdots\cdots & r_{p-1,p+1} & \\ r_{p,1} & r_{p,2} & r_{p,3} & \cdots\cdots & r_{p,p+1} \end{bmatrix} \tag{13}$$

$$\bar{\mathcal{R}} = \begin{bmatrix} r_{1,1}+jr_{1,2} & r_{1,3}+jr_{1,4} & \cdots\cdots & r_{1,p}+jr_{1,p+1} & \\ r_{2,1}+jr_{2,2} & r_{2,3}+jr_{2,4} & \cdots\cdots & r_{2,p}+jr_{2,p+1} & \\ \vdots & \vdots & \vdots & \cdots\cdots & \vdots \ \vdots \\ \vdots & \vdots & \vdots & \cdots\cdots & \vdots \ \vdots \\ r_{p-1,1}+jr_{p-1,2} & \cdots\cdots & r_{p-1,p}+jr_{p-1,p+1} & & \\ r_{p,1}+jr_{p,2} & \cdots\cdots & r_{p,p}+jr_{p,p+1} & & \end{bmatrix} \tag{14}$$

Complex matrix construction is made for a purpose of increasing bit per Hertz of mapping before resizing mapped data.

Step 9. Resize the matrix $\overline{R}$ to a one dimensional vector $r(k)$ of length $p \times (p+1)/2$.

$$r(k) = \left(r_0 r_1 r_2 \cdots r_{p(p+1)/2}\right)^T \tag{15}$$

Step 10. Take the 1D-IFFT for the vector, $r(k)$ to obtain the sub-channel modulation.

$$s(k) = \frac{1}{p(p+1)/2} \sum_{k=0}^{N_C-1} r(k) e^{\frac{j2\pi kn}{p(p+1)/2}} \tag{16}$$

where N_C number of carriers.

Step 11. Finally, convert the vector $s(k)$ to serial data symbols: $s_0, s_1, s_2, \ldots, s_n$. An illustrative numerical example of converting binary data to constellated data using 2-Radon mapping is provided below.

$$\begin{bmatrix} 1 \\ 0 \\ 1 \\ 1 \\ 0 \\ 1 \\ 1 \\ 1 \\ 0 \end{bmatrix} \xrightarrow[\text{1DVector to 2DMatrix}]{\text{InputFrame}} \begin{bmatrix} 1 & 1 & 1 \\ 0 & 0 & 1 \\ 1 & 1 & 0 \end{bmatrix}$$

$$\xrightarrow{\text{2DFFT}} \begin{bmatrix} 6.0000 & 0 & 0 \\ (1.5000+0.8660i) & (1.5000+0.8660i) & (-1.5000+0.8660i) \\ (1.5000-0.8660i) & (-1.5000-0.8660i) & (1.5000-0.8660i) \end{bmatrix} \xrightarrow{\text{Optimal ordaring}}$$

$$\begin{bmatrix} 6.0000 & 6.0000 & 6.0000 \\ (1.5000+0.8660i) & (1.5000+0.8660i) & (-1.5000-0.8660i) \\ (1.5000-0.8660i) & (1.5000-0.8660i) & (-1.5000+0.8660i) \end{bmatrix}$$

$$\xrightarrow{\text{1DIFFT}} \begin{bmatrix} 3.000 & 3.000 & 2.000 & 1.000 \\ 1.000 & 1.000 & 2.000 & 3.000 \\ 2.000 & 2.000 & 2.000 & 2.000 \end{bmatrix}$$

$$\xrightarrow[\text{Normalized by } 1/\sqrt{3}]{\text{p=3}} \begin{bmatrix} 1.7321 & 1.7321 & 1.1547 & 0.5774 \\ 0.5774 & 0.5774 & 1.1547 & 1.7321 \\ 1.1547 & 1.1547 & 1.1547 & 1.1547 \end{bmatrix}$$

$$\xrightarrow{\text{Create Constellate data}} \begin{bmatrix} 1.7321 + 1.7321i & 1.1547 + 0.5774i \\ 0.5774 + 0.5774i & 1.1547 + 1.7321i \\ 1.1547 + 1.1547i & 1.1547 + 1.1547i \end{bmatrix}$$

$$\xrightarrow{\text{2D Matrix to 1D Vector}} \begin{bmatrix} 1.7321 + 1.7321i \\ 0.5774 + 0.5774i \\ 1.1547 + 1.1547i \\ 1.1547 + 0.5774i \\ 1.1547 + 1.7321i \\ 1.1547 + 1.1547i \end{bmatrix} \xrightarrow{\text{Mapped Frame}}$$

In the above procedure Step 2 divides the number of data points by $N/2$ and also Step 8 divides the number of data points by two i.e. this process divides the number of data points by N and that is equivalent to 2^N-QAM map from spectral efficiency point of view. Hence 4-Radon is equivalent to 16-QAM and 6-Radon is equivalent to 64-QAM etc.

The N-Radon demapper (demodulation) for Fig. 4 is performed by taking the inverse operations of Fig. 5. Which means converting the matrix with complex numbers of size $\{p, (p+1)/2\}$ from 1D to 2D matrix, then generating matrix of real numbers by placing the real numbers in the first column of the complex matrix in the first column of the real matrix and the imaginary numbers in the first column of the complex matrix in the second column of the real matrix and so on, so as at the end, the real matrix will be of dimension $(p, p+1)$. Multiplying the real matrix by square root of p and taking 1D-FFT for each column then taking optimal reordering to obtain matrix of dimension (p, p). After that taking 2D IFFT and converting the resultant matrix from 2D to 1D, the length of resultant vector is (p^2). Now multiply this vector by k (which equal to square root of 3 in case of 4-Radon, and equal to square root of 7 in case of 6-Radon map), and correct the numbers in the last vector by using a suitable decision thresholds (0.5, 1.5, 2.5). So at the end of this step all elements will be between (0 and $2^{N/2} - 1$). Now convert this element from decimal to binary, to obtain matrix of dimension $\left(p^2, N/2\right)$, and by converting this matrix from 2D to 1D, the N-Radon demapper will be completed, and the final vector will be of length $(N/2)\, p^2$.

The performances of 2-Radon mapper, QPSK, and 16-QAM were simulated using MATLAB and the results of simulation are shown in Fig. 6. From which it can be seen that 2-Radon mapper gives a gain in SNR more than 3 dB to achieve a BER performance of 10^{-4} as compared with standard QPSK and more than 10 dB as compared with 16-QAM in Additive White Gaussian Noise (AWGN) channel and 4-Radon mapper gives a gain in SNR about 3 dB over the 16-QAM mapper to achieve the same BER performance.

4 Simulation and Performance Analysis of 4-Radon and 6-Radon Based OFDM Transceiver

As an examples of N-Radon based OFDM, in this section we provide and discuss the obtained performance results of proposed 4-Radon and 6-Radon based OFDM systems simulations.

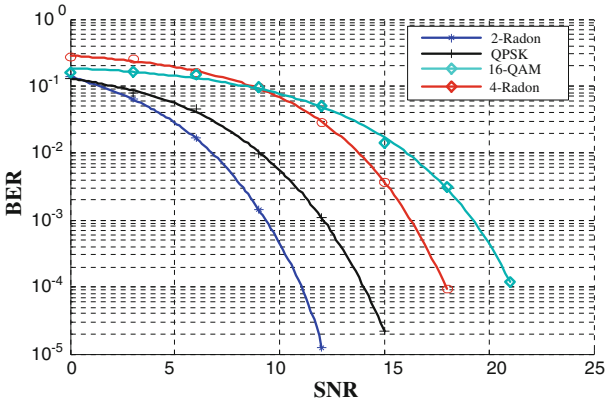

Fig. 6 Performance of Radon QAM mappers in AWGN channel

Theoretical performance analysis and derivations of proposed systems are not discussed in this paper; it will be a subject of the next work which is the continuation of this one. The methodology and the principle of BER formulation for such problems can be found in references such as [27–29].

Because 4-Radon mapping is equivalent to 16-QAM mapping and 6-Radon mapping is equivalent to 64-QAM mapping from spectral efficiency point of view, the performances of the 4-Radon mapping OFDM in different channel conditions are compared with the performances of the 16-QAM map OFDM. Also the performances of the 6-Radon map OFDM are compared with the performance of the 64-QAM mapping OFDM. The simulations are performed for a frame-based un-coded system. Three types of channels are used AWGN, multi-path Raleigh distributed flat-fading, and multi-path Raleigh distributed selective-fading. The selective-fading channel is simulated as 1-D FIR filter that adds multi-path effect and AWGN to transmitted symbols. The channel is assumed to be slowly varying, which doesn't change within a packet frame. Thus, the estimation is done with the long preambles at the beginning of the frame. The channel frequency response is estimated by using training and received sequences as follows: $H(k) = \frac{Received\ Training\ Sample(k)}{Transmitted\ Training\ Sample\ (k)}, k = 0, 1, 2, \ldots$ The channel frequency response is used to compensate the channel effects on the data, and the estimated data is found using the following equation: $Estimated - data(k) = H^{-1}_{estimate}(k) * Received - data(k), k = 0, 1, 2, \ldots$ The system uses 64-point FFT, 7 by 7 FRAT window i.e. $p = 7$. The OFDM frame duration worth's 80 chips where 64 are for data while 16 are cyclic prefix. Out of the 64 narrow-band sub-carriers, only 52 are carrying signal and other 12 are zeros (guard or null sub-carriers). Four of the 52 sub-carriers are used as pilots and the other 48 are used for data. The same parameters and channel types are used in the simulation for the proposed 4-Radon and 6-Radon based OFDM systems and the conventional OFDM systems.

The BER performance of 4-Radon OFDM and 16-QAM OFDM in AWGN channel are provided in Fig. 7. It can be seen that the 4-Radon OFDM is better than 16-QAM OFDM. It requires less SNR (about 5 dB) to achieve a BER performance of 10^{-4} as compared with standard 16-QAM based OFDM.

In Fig. 8 are provided the BER performance of 4-Radon OFDM and 16-QAM OFDM in flat fading channel. Again the 4-Radon OFDM is better than 16-QAM OFDM, and it has about 7 dB SNR advantage at BER equal 10^{-4}. Figure 9 shows the performance in selective fading channel with 2nd path signal of delay 4 samples and gains equal -10.5 dB. The

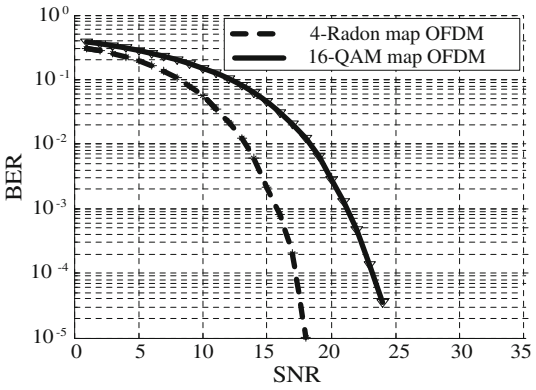

Fig. 7 BER performance of 4-Radon OFDM and 16QAM OFDM in AWGN channel

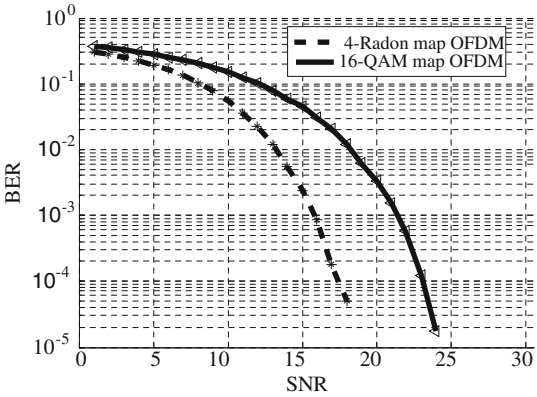

Fig. 8 BER for 4-Radon OFDM and 16-QAM OFDM in flat fading channel

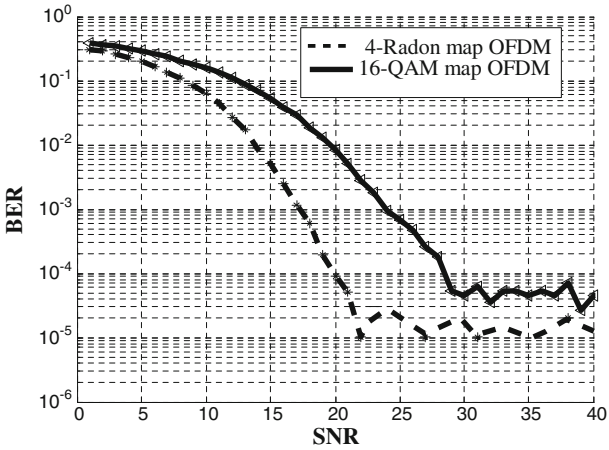

Fig. 9 BER for 4-Radon OFDM and 16-QAM OFDM in selective fading channel

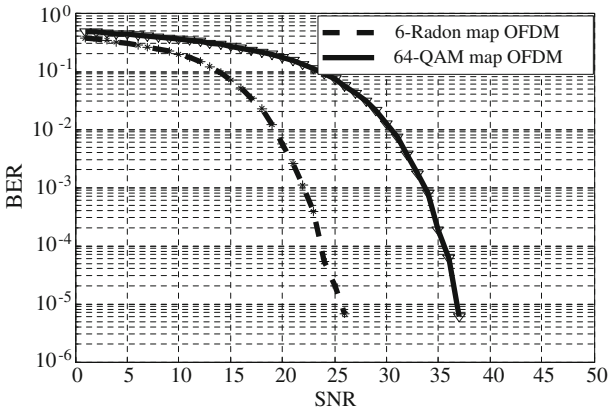

Fig. 10 BER for 6-Radon OFDM and 64-QAM OFDM in AWGN channel

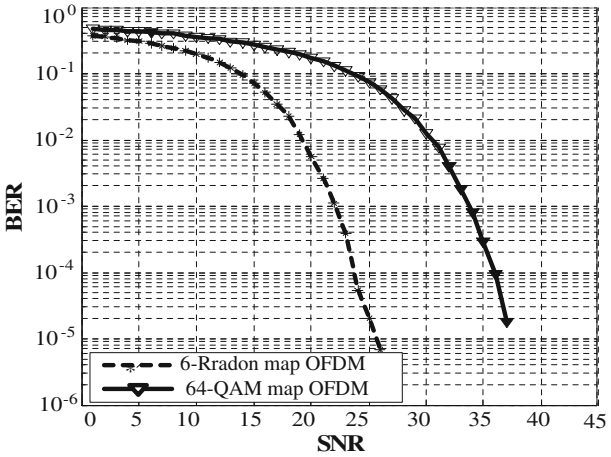

Fig. 11 BER for 6-Radon OFDM and 64-QAM OFDM in flat fading channel

4-Radon OFDM has about 7 dB advantage in SNR as compared with the standard 16-QAM based to achieve a BER performance of 10^{-4}.

Figures 10, 11 and 12, show the performance of 6-Radon mapping OFDM as compared with 64-QAM mapping OFDM, with different channel models. In all these figures the 6-Radon mapping OFDM has a SNR advantage over 64-QAM to achieve the same performance. The 6-Radon OFDM gives a gain in SNR about 11.5 dB to achieve a BER performance of 10^{-3}as compared with the standard 64-QAM OFDM.

Peak to Average Power Ratio (PAPR) is an important parameter for OFDM systems. It was defined as the peak signal power versus the average signal power [30]. In general PAPR is a random variable for each OFDM symbol. The large amplitude samples are clipped in the power amplifiers which results in a harmonics in the carrier frequencies, and a large bandwidth for OFDM signal due to large side lobes and out-of-band distortion power [30–32].

The average PAPR for many OFDM symbols was measured using Eq. (17) at a number of useful sub-carriers equals 28.

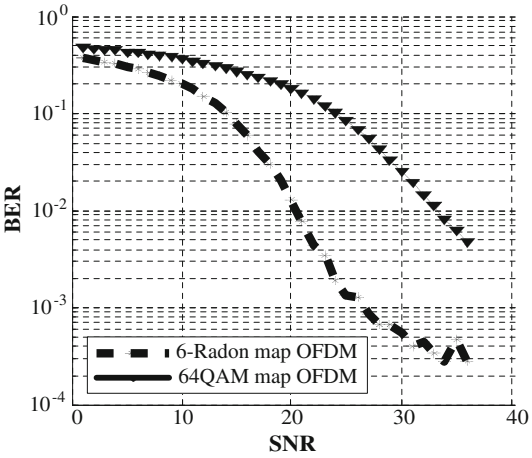

Fig. 12 BER for 6-Radon OFDM and 64-QAMOFDM in selective fading channel

$$PAPR = \frac{\max\left\{|X_i|^2\right\}}{E\left\{|X_i|^2\right\}} \tag{17}$$

where X_i - is the ith bit in an IFFT output stream, E {}- the expected value operation.

The value of PAPR was 10.7786 dB for 4-Radon-based OFDM, 12.5271 dB for 16-QAM based OFDM, 11.1712 dB for 6-Radon-based OFDM, and 12.8286 dB for 64-QAM based OFDM. It can be seen from these results that PAPR for Radon based-OFDM is less than that for standard FFT-OFDM. Also simulations of time domain signal envelopes show that Radon-based OFDM has less peaks of large amplitude compared with QAM-OFDM which is the reason for the PAPR results.

5 The Effect of Channel Parameters and Cyclic Prefix Variation on Proposed System Performance

The effect of selective fading channel parameters (2nd path gain and 2nd path signal delay) variation on the BER performance of the proposed system is studied. Figure 13 illustrates the BER performance of 4-Radon, 16-QAM, 6-Radon and 64QAM OFDM systems as a function of second path gain keeping SNR = 18 dB, 2nd path delay equal 8 samples and Doppler frequency equal 100 Hz. As expected Fig. 13 shows the performance decreasing with increasing second path gain, however, it can be seen that the performance of proposed systems is better than conventional systems for all values of second path gain.

Figure 14 shows the BER performance of 4-Radon, 16-QAM, 6-Radon and 64QAM OFDM systems as a function of second path delay in a selective fading channel. The delay varies from 1 to 15 samples. During this simulation the SNR is fixed to 18 dB, the 2nd path gain is equal to −8 dB and the Doppler frequency is equal 100 Hz. From Fig. 14 it is seen that in general the BER performance increase with increasing the 2nd path delay for all systems, however, the increment in Radon based-OFDM systems is larger than that of conventional QAM based-OFDM systems.

Figure 15 shows the BER performance of the 4-Radon OFDM and 16-QAM OFDM for various values of cyclic prefix (CP). A CP of 6.25, 12.5, and 25% which are equivalent to 4,

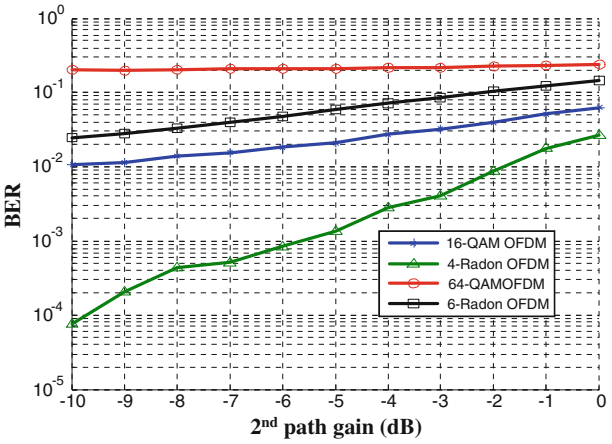

Fig. 13 Effect of second path gain of selective fading channel on system BER performance

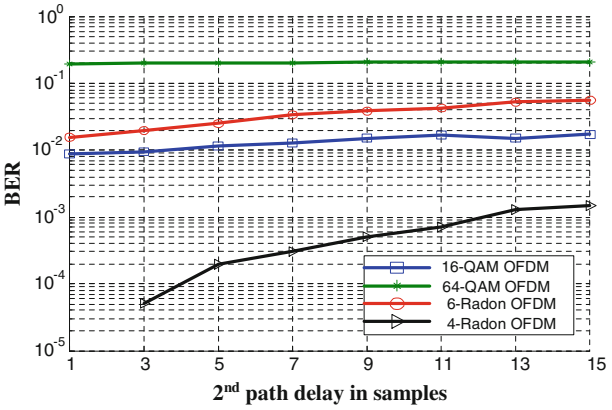

Fig. 14 Effect of second path delay of selective fading channel on system BER performance

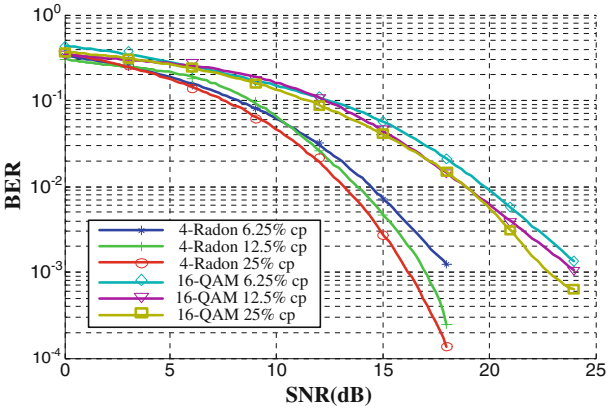

Fig. 15 BER performance of OFDM systems for various CP

8, 16, samples respectively are considered. Channel parameters are kept constant: Doppler frequency equal 100 Hz, 2nd path delay equal 8 samples (CP = 6.25%), and 2nd path gain equal −8 dB. It is observed that the first case (CP = 6.25% ≡ 4 samples) is affected more than the others, because ISI affects the first case while it does not appear in the other two types because the CP is greater than the delay spread of 2nd path. This means that BER performance is improved with increasing the CP while it degrades the bit rate.

6 Conclusions

In this paper a new generalized N-Radon based OFDM method is used as a data mapping to replace the QPSK, 16-, 64-, 256-, 1024-QAM, etc. Proposed method improves the performance of OFDM system and reduces the required energy for mapping. This method does not require complex processing except some 1D and 2D FFT algorithms. From the results of simulation, the proposed 4-Radon mapping OFDM gives about 5 dB gain in SNR as compared with the 16-QAM mapping OFDM to achieve BER equal 10^{-4} in AWGN and flat fading channels. Also the proposed 4-Radon mapping OFDM gives a gain in SNR of about 7 dB as compared with the 16-QAM mapping OFDM in selective fading channel. The performance is improved, due to implementing IFFT twice: in the data mapping and in the sub-carrier modulation, which increases the orthogonality. The optimal ordering (best direction) in the Radon mapper can be considered as a good interleaver which serves in error spreading. Also it was found that the effect of channel parameters and cyclic prefix variation on proposed system performance is less than that for conventional OFDM system. The obtained results show that PAPR for Radon based-OFDM is less than that for standard FFT-OFDM and Radon-based OFDM has less peaks of large amplitude compared with QAM-OFDM which is the reason for the PAPR results.

References

1. Shin, O. S., Chan, A. M., Kung, H. T., & Tarokh, V. (2007). Design of an OFDM cooperative space-time diversity system. *IEEE Transactions on Vehicular Technology, 56*(4), 2203–2215.
2. Al-Dhahir, N., & Cioffi, J. M. (1996). Optimum finite-length equalization for multicarrier transceivers. *IEEE Transactions on Communications, 44*(1), 56–64.
3. Zhang, H., Yuan, D., & Pätzold, M. (2007). Novel study on PAPRs reduction in wavelet-based multicarrier modulation systems. Elsevier Inc, *Digital Signal Processing, 17*, 272–279.
4. Weinstein, S., & Ebert, P. (1971). Data transmission by frequency division multiplexing using the discrete fourier transform. *IEEE Transaction on Communication Technology, COM-19*, 628–634.
5. Nghi, N. H., & Nguyen, H. H. (2007). IEEE, and Tho Le-Ngoc Bit-interleaved coded OFDM with signal space diversity: Subcarrier grouping and rotation matrix design. *IEEE Transactions on Signal Processing, 55*(3), 1137–1149.
6. Lawrey, E. (Oct 1997). The Suitability of OFDM as a modulation technique for wireless telecommunications, with a CDMA Comparison. Thesis, James Cook University.
7. Jeon, W. G., Chang, K. H., & Cho, Y. S. (1999) An equalization technique for orthogonal frequency-division multiplexing systems in time-variant multipath channels. *IEEE Transactions On Communications, 47*(1), 27–32.
8. Nee, R. V., & Prasad, R. (2000). *OFDM for wireless multimedia communications*. London, UK: Artech House.
9. Koffman, I., & Roman, V. (2002). Broadband wireless access solutions based on OFDM access in IEEE 802.16. *IEEE Communications Magazine, 40*(4), 96–103.
10. Lee, I., Chow, J. S., & Cioffi, J. M. (2007). Performance evaluation of a fast computation algorithm for the DMT in high-speed subscriber loop. *IEEE Journal on Selected Areas in Communications, 13*(9), 1564–1570.

11. Prasad, R. (2004). *OFDM for Wireless Communications Systems*. London, UK: Artech House.
12. Batra, A., Balakrishnan, J., Aiello, G. R., Foerster, J. R., & Dabak, A. (2004). Design of multiband OFDM system for realistic UWB channel environments. *IEEE Transaction on Microwave Theory And Techniques, 52*, 2123–2138.
13. Cimini, L. J., Jr. (1985). Analysis and simulation of a digital mobile channel using orthogonal frequency division multiplexing. *IEEE Transactions on Communications, COM-33*, 665–675.
14. Zhao, Y., & Haggman, S.-G. (2001). Intercarrier interference self-cancellation scheme for OFDM mobile communication systems. *IEEE Transactions on Communications, 49*(7), 1185–1191.
15. Tomasin, S., Gorokhov, A., Yang, H., & Linnartz, J.-P. (2005). Iterative interference cancellation and channel estimation for mobile OFDM. *IEEE Transactions On Wireless Communications, 4*(1), 238–245.
16. Deans, S. R. (1983). *The Radon transform and some of its applications*. New York: Wiley.
17. Bolker, E. D. (1987). The finite Radon transform. In S. Helgason, R. L. Bryant, V. Guillemin, & R. O. Wells Jr. (Eds.), *Integral geometry, AMS contemporary mathematics* (Vol. 63, pp. 27–50).
18. Beylkin, G. (1983). Discrete Radon transforms. *IEEE Transactions on Acoustic, Speech and Signal Processing, ASSP-35*, 162–172.
19. van den Boogaart, K. G., Hielscher, R., Prestin, J., & Schaeben, H. (2006). Kernel-based methods for inversion of the Radon transform on SO(3) and their applications to texture analysis. *Journal of Computational and Applied Mathematics, 199*(1), 122–140.
20. Courmontagne, P. (2005). An improvement of ship wake detection based on the Radon transform. *Signal Processing, 85*(8), 1634–1654.
21. Coetzer, J., Herbst, B. M., & du Preez, J. A. (2004). Offline signature verification using the discrete Radon transform and a hidden Markov model. *EURASIP Journal on Applied Signal Processing, 2004*(1), 559–571.
22. Wang, X., Xiao, B., Ma, J.-F., & Bi, X.-L. (Dec 2007). Scaling and rotation invariant analysis approach to object recognition based on Radon and Fourier-Mellin transforms. *Pattern Recognition, 40*(12), Elsevier Science Inc.
23. Tsuboi T., & Hirai, S. (2006). Detection of planar motion objects using Radon transform and one-dimensional phase-only matched filtering. *Systems and Computers in Japan, 37*(5), Wiley-Inter-science.
24. Al-Jawhar, W., Kattoush, A. H., Abbas, S. M., & Shaheen, A. T. (2008). A high speed high performance parallel Radon based OFDM transceiver design and simulation. Elsevier, *Digital Signal Processing, 18*, 907–918.
25. Do, M. N., & Vetterli, M. (2003). The finite ridgelet transform for image representation. *IEEE Transactions on Image Processing, 12*(1), 16–28.
26. Natterer, F. (1989). *The mathematics of computerized tomography*. New York: Wiley.
27. Hu, J., & Beaulieu, N. C. (2008). Accurate closed-form approximations for the performance of equal gain combining diversity systems in Nakagami fading channels. *European Transactions on Telecommunications, 19*, 707–717.
28. Le, K. N. BER of OFDM in Rayleigh fading environments with selective diversity. *Wireless Communications and Mobile Computing*, (in press), doi:10.1002/wcm.775.
29. Le, K. N. (2008). Insights on ICI and its effects on performance of OFDM systems. *Digital Signal Processing, 18*(6), 876–884.
30. Mestdagh, D., & Spruyt, P. (1996). A method to reduce the probability of clipping in DMT-based transceivers. *IEEE Transactions on Communication, 44*(10), 1234–1238.
31. Müller, S., Bäuml, R., Fischer, R., & Huber, J. (1997). OFDM with reduced peak-to-average power ratio by multiple signal representation. *Annals of Telecommunications, 52*(1–2), 58–67.
32. Wulich, D., & Goldfeld, L. (1999). Reduction of peak factor in orthogonal multicarrier modulation by amplitude limiting and coding. *IEEE Transactions on Communication, 47*(1), 18–21.

Author Biographies

Abbas Hasan Kattoush received his M.S., and Ph.D. degrees in communication Eng. from USSR in 1979 and 1984 respectively. For 10 years Dr. Kattoush was a technical manager of a leading SAKHER computers company. He was a pioneer in computer networking and software engineering in Jordan. From 1993 to 2000 he worked at Applied Science University Amman Jordan where he was a founding member and a head of the department of electrical and computer engineering. In 2000 Dr. Kattoush moved to Al-Isra University, Amman-Jordan where he worked as an associate professor and a head of department of Electrical and Computer Engineering until October 2008. Currently he is an associate professor and a head of department of Electrical and Computer Engineering at Tafila Technical University, Tafila-Jordan. His areas of research interest include DSP, digital communication systems, phase unwrapping, interferometric SAR image analysis, filtering, and interpretation. He has authored several tenths of research articles, textbooks, and computer software systems.

Waleed Ameen Mahmoud Al-Jawher Dean of Engineering College, University of Isra, Jordan. He received a School of Research in Digital Signal Processing (2005). He received his Ph.D. in Digital Signal Processing from University of Wales University College of Swansea, United Kingdom (1986). He has a teaching experience in engineering for 32 years. A total of (15) National Awards. He Published over (224) papers, Supervised (202) M.Sc. and Ph.D. Students. He was the First professor Award of University of Baghdad, the First professor Award of the Ministry of Higher Education & Scientific Research of Iraq (National first Professor Award). His present areas of research interest are the field of DSP and Communication.

Sulaiman M. Abbas was born in 1951. He received his B.Sc. from Baghdad University in 1972; and his M.Sc. from Birmingham University in 1978. He is a lecturer in the Department of Electronic Engineering, College of Engineering, University of Baghdad (1979); Assistant professor in 1988. Currently he is the head of the Department of Electrical Engineering at University of Baghdad. His areas of research interest include fields in solid state electronics and communication engineering.

Ali Tweij Shaheen was born in Baghdad in 1978. He received his B.Sc. in Electrical Engineering from University of Baghdad in 2000, and his M.Sc. in electronic and communication from University of Baghdad 2007. He is working as a lecturer in the electrical engineering department in the University of Baghdad. His areas of research interest are the field of DSP and Communication.